Network Pharmacology and Molecular Docking Analysis of *Allium tuberosum*-Derived Bioactive Compounds as Potential Therapeutic Agents for Malaria

Kiky Martha Ariesaka[1,*] and Moh. Mirza Nuryady[2,3]

[1] Department of Medicine, Faculty of Medicine, State University of Malang, Indonesia
[2] Institute of Parasitology, Department of Biological Science and Pathology, Veterinary Medicine of Vienna, Austria
[3]Biology Education Department, Faculty of Education, Science and Humanities, University of Muhammadiyah Malang, Indonesia
kiky.martha.fk@um.ac.id

Abstract. Malaria remains a major global health burden amid rising concerns over artemisinin resistance, highlighting the need for new antimalarial candidates with broader mechanisms of action. This study aimed to identify the antimalarial potential of *Allium tuberosum* phytoconstituents through an integrated network pharmacology and AI-assisted molecular docking approach. A total of 45 bioactive compounds were retrieved from the KNAPSACK database, of which 7 compounds met the ADMET screening criteria. Network pharmacology identified 88 shared targets between *A. tuberosum* and malaria-associated genes, with STAT3 selected as the primary hub gene based on CytoHubba MCC analysis. GO and KEGG enrichment analyses revealed significant involvement of oxidative stress response, nuclear receptor signaling, IL-17 signaling, and arginine metabolism pathways relevant to malaria pathogenesis. AlphaFold2 predicted a STAT3 structure with a mean pLDDT of 83.8 and a pTM of 0.698, subsequently used for DiffDock-L binding pocket prediction and molecular docking. C7 showed the strongest binding affinity toward STAT3 (S-score −13.2736 kcal/mol), outperforming the reference compound (−8.5137 kcal/mol) through hydrogen bond interactions with GLU357 and GLN448 within the STAT3 SH2 domain. These findings suggest that *A. tuberosum* bioactive compounds, particularly C7, has potential to be candidate antimalarial agents targeting STAT3-mediated inflammatory pathways. Further in vitro and in vivo validation is required to confirm these findings.

Keywords: *Allium tuberosum*, enrichment analysis, malaria, molecular docking, network pharmacology.

1 Introduction

Malaria remains a serious global health problem. It is caused by infection with parasites of the genus Plasmodium, transmitted through the bite of female Anopheles

© The Author(s) 2026
K. M. Ariesaka and D. Fauziah (eds.), *Proceedings of the 3rd Malang International Conference on Medical and Health Sciences (MICROMEDHS 2026)*, Advances in Health Sciences Research 96,
https://doi.org/10.2991/978-94-6239-807-8_5

mosquitoes. The World Malaria Report 2025 recorded approximately 282 million malaria cases and 610,000 deaths worldwide [1].

Current first-line therapy for malaria generally relies on artemisinin-based combination therapy (ACT). ACT has proven effective in rapidly reducing parasitemia, but parasite resistance to artemisinin has been confirmed or suspected in several countries [2, 3]. This resistance threatens the effectiveness of standard therapies and has the potential to delay the achievement of global malaria elimination targets [1]. Furthermore, malaria involves complex pathogenic mechanisms, including host immune responses, inflammatory processes, and molecular interactions between parasites and host cells [4]. This situation often makes single-target therapeutic approaches less effective in addressing the complexity of this disease. Therefore, exploration of new antimalarial agent candidates with broader mechanisms of action is urgently needed.

Medicinal plants have long been an important resource in modern drug development due to their diverse secondary metabolite content [5]. One plant with potential for development is *Allium tuberosum* (chives), a member of the Amaryllidaceae family rich in organosulfur compounds, flavonoids, terpenoids, and essential oils [6]. Various studies have reported that compounds in *A. tuberosum* have antioxidant, antimicrobial, anti-inflammatory, and anticancer activities [6–8]. The multicomponent nature of these natural products makes conventional pharmacological approaches that focus on a single drug-target relationship inadequate to comprehensively elucidate their mechanisms of action. However, to date, research specifically exploring the potential of *A. tuberosum* phytoconstituents as candidate antimalarial agents remains very limited [9]. The key molecular targets and biological mechanisms underlying the possible antimalarial effects of *A. tuberosum* compounds are also poorly understood. This research gap highlights the need for approaches that systematically integrate the relationships between bioactive compounds, protein targets, and disease pathways [17].

Network pharmacology has been widely used to uncover interactions between bioactive compounds, protein targets, and disease at the systems level [10]. Developments in artificial intelligence (AI) technologies, such as AlphaFold2 and DiffDock, enable the prediction of protein structures and protein-ligand interactions with greater accuracy and efficiency than conventional approaches [11]. To the best of authors' knowledge, no study has integrated network pharmacology and AI-based molecular docking to explore the antimalarial potential of *A. tuberosum*. Therefore, this study aims to identify key bioactive compounds from *A. tuberosum*, determine potential molecular targets related to malaria through network pharmacology, and evaluate their affinity and interaction patterns using AI-based molecular docking. The results of this study are expected to provide a scientific basis for the development of candidate therapeutic agents based on natural ingredients to support malaria elimination efforts in the future.

2 Materials and Methods

2.1 Bioactive Compounds Identification

A. tuberosum phytoconstituents were collected from the KNAPSACK database. The chemical structures and Simplified Molecular Input Line Entry System (SMILES) notation of each compound were then obtained from the PubChem database. These data served as the basis for further analysis.

2.2 ADMET Prediction and Screening

The pharmacokinetic and toxicity profiles of the identified phytoconstituents were evaluated using the DeepPK platform. Compounds with predicted oral bioavailability values ≥20% were retained for further analysis. Only compounds with a "Safe" classification for Ames mutagenicity, carcinogenesis, drug-induced liver injury (DILI I and II), and hERG blocker toxicity were selected for the next stage.

2.3 Compound-Related Target Prediction

Potential protein targets of the selected compounds were predicted using SwissTargetPrediction. SMILES notation was used as input, and only targets with a predicted probability greater than 0.05 were included in further analysis.

2.4 Malaria-Related Target Identification

Malaria-related genes were collected from the GeneCards database using the keyword "malaria." Only protein-coding genes were retained, and targets with a relevance score greater than 5.0 were selected. Duplicate data were removed before further analysis.

2.5 Shared Target Identification and Compound-Target Network Construction

Intersections between compound targets and malaria-related genes were identified using Venny 2.1. The overlapping genes were considered potential therapeutic targets of A. tuberosum against malaria and were subsequently imported into Cytoscape version 3.10.4 for network visualization and analysis.

2.6 Protein-Protein Interaction Network Analysis

Protein-protein interaction (PPI) analysis was performed using STRING with *Homo sapiens* as the reference organism. The minimum interaction score was set at 0.700 (high confidence). The resulting interaction network was exported and visualized using Cytoscape version 3.10.4.

Hub genes were identified using the CytoHubba plugin. The Degree algorithm was used to rank target genes based on their relative importance in the interaction network. The highest-ranking gene was designated as the hub gene.

2.7 GO and KEGG Pathway Enrichment Analysis

Gene Ontology (GO) enrichment analysis, including Biological Process (BP), Molecular Function (MF), and Cellular Component (CC), as well as Kyoto Encyclopedia of Genes and Genomes (KEGG) pathway enrichment analysis, was performed using ShinyGO version 0.85. The false discovery rate (FDR) threshold was set at 0.05. The 20 pathways with the highest significance were retained for visualization.

2.8 AI-Assisted Protein Structure Modeling and Binding Pocket Prediction

The complete amino acid sequence of the hub gene, STAT3 (UniProt: P40763), was obtained from UniProt. Three-dimensional protein structure prediction was performed using AlphaFold2 with default parameters. The model with the highest confidence level (Rank 1) was selected for further analysis.

Potential ligand binding regions were identified using DiffDock-L, available through the NeuroSnap AI platform. The AlphaFold2 Rank 1 predicted STAT3 structure was used as the receptor, while the reference compound (PubChem CID: 2779853) served as a STAT3 comparison inhibitor. The protein-ligand complex with the highest confidence score was selected and exported in Structure Data File (SDF) format.

2.9 Molecular Docking

Receptor and ligand preparation was performed using the Molecular Operating Environment (MOE) version 2019.01. Conformation searches were performed using the LowModeMD algorithm. Subsequent protonation and energy minimization were performed with default settings.

Molecular docking simulations were performed using the Dock module in MOE. Initial ligand placement was performed using the Triangle Matcher algorithm and assessed using the London dG scoring function. The resulting poses were then refined using the Induced Fit protocol and reassessed using London dG. The best binding conformation was selected based on the lowest docking score (S-score) and the best interaction.

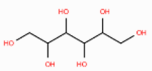
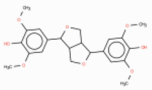
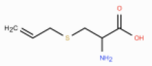
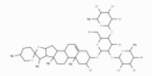
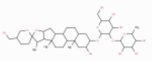
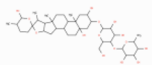
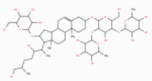
3 Results and Discussion

3.1 Screening of Active Compounds and ADMET Analysis

A total of 45 phytoconstituents of *A. tuberosum* were successfully collected from the KNAPSACK database. ADMET screening process using the DeepPK platform was

then performed on all these compounds. Seven compounds met the criteria for oral bioavailability ≥20% and were classified as safe for Ames mutagenicity, DILI, and hERG blocker (Table 1). Most of the selected compounds belonged to the steroidal saponin (Tuberoside) group, followed by one lignan and one organosulfur compound.

Table 1. ADMET properties of selected phytoconstituents from *Allium tuberosum*

Compound	Structure	Human Oral Bioavailability 20%	Fraction Unbound	Plasma Protein Binding	CYP Inhibitor	Half-life	Toxicity (carcinogenesis, DILI II, hERG)
C1		0.582	0.4	-4.98	-	>= 3hs	Safe
C2		0.692	0.93	18.88	2C19	< 3hs	Safe
C3		0.728	0.53	0.64	-	>= 3hs	Safe
C4		0.824	0.81	3.49	-	< 3hs	Safe
C5		0.857	0.85	11.85	-	< 3hs	Safe
C6		0.832	0.68	1.85	-	< 3hs	Safe
C7		0.65	0.67	-11.3	-	< 3hs	Safe

3.2 Network Pharmacology Analysis

Potential protein targets of the seven selected compounds were predicted using SwissTargetPrediction, resulting in 197 unique targets. Malaria-related genes were collected from GeneCards, resulting in 2,262 genes after filtration. Intersections between the two datasets were identified using Venny 2.1, resulting in 88 shared targets between *A. tuberosum* and malaria (Fig. 1). These shared targets were considered potential therapeutic targets of *A. tuberosum* against malaria and were used for further network analysis.

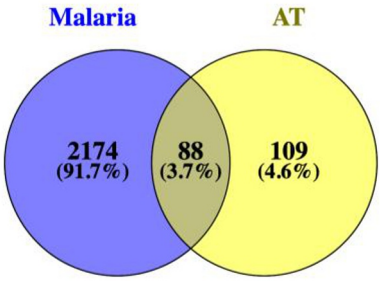


Fig. 1. Venn diagram showing the overlap between *A. tuberosum* (AT)-related targets and malaria-associated genes.

3.3 Protein–Protein Interaction Network and Hub Gene Identification

Protein–protein interaction analysis of the 88 shared targets resulted in a network with 88 nodes and 175 edges (Fig. 2a). The average node degree was recorded at 3.98, with an average local clustering coefficient of 0.44. The PPI enrichment p-value was recorded at less than 1.0×10^{-16}, indicating that the formed network contained significantly more interactions than would be expected randomly. This finding indicates that these targets are biologically closely related, rather than isolated.

Hub gene identification using CytoHubba with the MCC algorithm yielded 10 genes with the highest topology scores: STAT3, HIF1A, HSP90AA1, MMP9, ESR1, AR, NR3C1, PTGS2, MMP2, and PPARG (Fig. 2b). These ten genes were closely connected to each other, indicating their central role in the network. Among these ten genes, STAT3 (Signal Transducer and Activator of Transcription 3) was selected as the primary hub gene for further analysis.

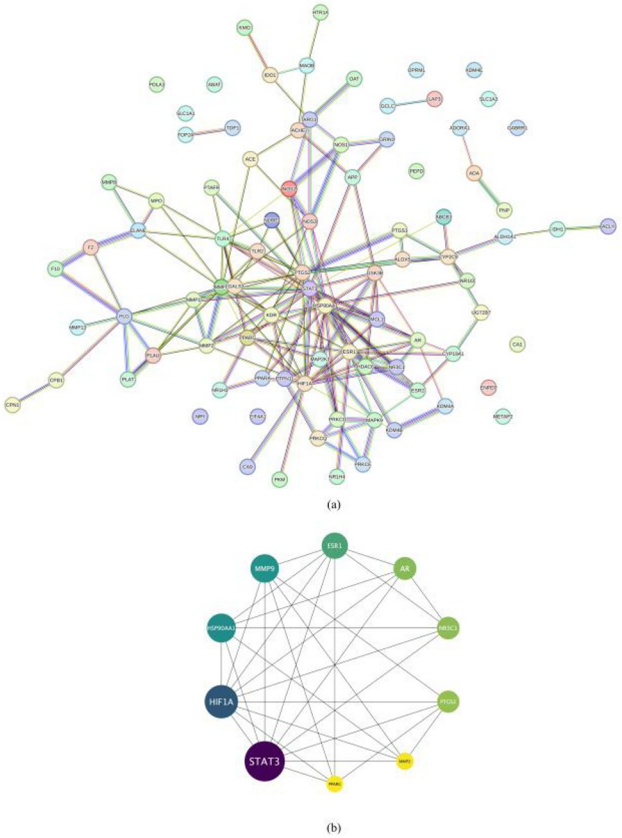


Fig. 2. PPI network and hub gene identification of the 88 overlapping targets. (a) Full PPI network constructed using the STRING database, where nodes represent proteins and edges indicate protein–protein interactions. (b) Top 10 hub genes ranked by Maximum Clique Centrality (MCC) showing a fully interconnected subnetwork centered on STAT3.

3.4 GO and KEGG Pathway Enrichment Analysis

Enrichment analyses of the 88 shared targets were performed using ShinyGO version 0.85 (Fig. 3). Among the enriched Biological Process terms, response to oxygen-containing compound and response to stress showed strong relevance to malaria pathogenesis, reflecting the oxidative stress generated during erythrocyte rupture and hemozoin release [12]. Response to lipid was also enriched, consistent with the disruption of host lipid metabolism that occurs during Plasmodium infection [13].

In the Cellular Component category, enrichment of cell surface, secretory vesicle, and extracellular space terms pointed to receptor-mediated host–parasite interactions and secreted inflammatory mediators, both of which underlie erythrocyte cytoadherence and immune cell activation during malaria infection [14].

For Molecular Function, nuclear receptor activity and ligand-activated transcription factor activity emerged as the most significantly enriched terms. This finding aligns with the presence of several nuclear receptor hub genes (PPARG, ESR1, AR, NR3C1), known to regulate macrophage polarization and anti-inflammatory responses during malaria infection [15]. Metallopeptidase activity was also enriched, corresponding to the MMP9 and MMP2 hub genes, both implicated in blood–brain barrier disruption during cerebral malaria [16].

KEGG pathway analysis identified the IL-17 signaling pathway, arginine biosynthesis, and arginine and proline metabolism as the pathways most relevant to malaria pathogenesis. Involvement of the IL-17 signaling pathway supports a role for Th17-mediated immunopathology during Plasmodium infection [17]. Arginine biosynthesis and arginine and proline metabolism are closely linked to nitric oxide production, whose depletion is strongly associated with endothelial dysfunction and severe malaria [13]. In addition, enrichment of the PD-L1 expression and PD-1 checkpoint pathway suggests a possible contribution to T cell exhaustion, a phenomenon well documented in chronic and severe malaria infection [18].

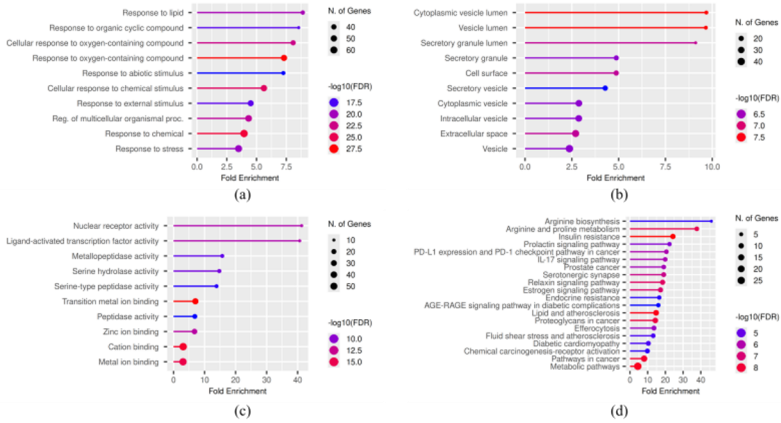


Fig. 3. GO and KEGG enrichment analyses of the 88 overlapping targets between *Allium tuberosum* and malaria. (a) Biological Process (BP), (b) Cellular Component (CC), (c) Molecular Function (MF), and (d) KEGG pathway enrichment results.

3.5 AI-Assisted Protein Structure and Binding Pocket Prediction

Three-dimensional structure prediction of STAT3 using AlphaFold2 produced five candidate models. The Rank 1 model, selected for subsequent analysis, showed a mean pLDDT of 83.8 and a pTM score of 0.698, indicating a reasonably high level of structural confidence for downstream docking analysis [19].

Binding pocket prediction using DiffDock-L on the Rank 1 STAT3 structure, with the reference compound (PubChem CID: 2779853) as ligand, generated a protein–ligand complex with a confidence score of 0.13. This predicted binding region was subsequently used as the docking reference site for the seven candidate compounds.

3.6 Molecular Docking Analysis

Molecular docking simulations showed that all seven candidate compounds successfully bound within the predicted STAT3 binding pocket (Table 2). C7 exhibited the strongest binding affinity, with an S-score of −13.2736 kcal/mol, followed by C6 (−12.2037 kcal/mol) and C4 (−11.2476 kcal/mol). The reference compound showed an S-score of −8.5137 kcal/mol. With the exception of C3 (−8.0573 kcal/mol), all tested compounds showed stronger predicted binding affinity toward STAT3 than the reference compound.

Table 2. Binding affinity (S-score) and interactions of the tested compounds against STAT3

Compound	RMSD	Binding affinity (kcal/mol)	Interacting Residue	Interaction Type	Distance (Å)	Energy (kcal/mol)
Ref. (CID: 2779853)	1.2985	−8.5137	GLU272	H-donor	3.33	−0.6
			GLN448	H-acceptor	2.49	−1.4
C1	-	−8.9552	GLU272	H-donor	3.26	−1.2
			GLU272	H-donor	3.19	−0.6
			GLU357	H-acceptor	3.05	−1.7
C2	-	−10.2486	HIS447 (5-ring)	H-pi	3.57	−0.5
C3	-	−8.0573	GLU272	H-donor	3.33	−1.3
			HIS447	H-acceptor	3.13	−1.3
C4	-	−11.2476	TYR446	H-donor	2.83	−1.4
C5	-	−10.5731	GLU357	H-acceptor	2.81	−1.7
C6	-	−12.2037	TYR446	H-donor	3.01	−1.0
			GLU357	H-acceptor	3.1	−1.6
			GLN279	H-acceptor	3.02	−1.0
C7	-	−13.2736	GLU357	H-donor	2.88	−2.3
			GLN448	H-acceptor	3.24	−0.7

Interaction analysis showed that C7 formed a hydrogen bond with GLU357 as a hydrogen-bond donor (distance 2.88 Å; energy −2.3 kcal/mol) and with GLN448 as a hydrogen-bond acceptor (distance 3.24 Å; energy −0.7 kcal/mol) (Fig. 4). Notably, GLN448 was also engaged by the reference compound, suggesting that C7 occupies an overlapping binding region within the STAT3 pocket. C6 additionally interacted with TYR446 and GLN279, while C4 interacted with TYR446. GLU357, TYR446, HIS447, and GLN279 are residues located within the SH2 domain of STAT3, a region essential for STAT3 dimerization and transcriptional activation. These findings suggest that the top-ranked compounds, particularly C7, C6, and C4 may interfere with STAT3 dimerization through occupation of this key regulatory region.

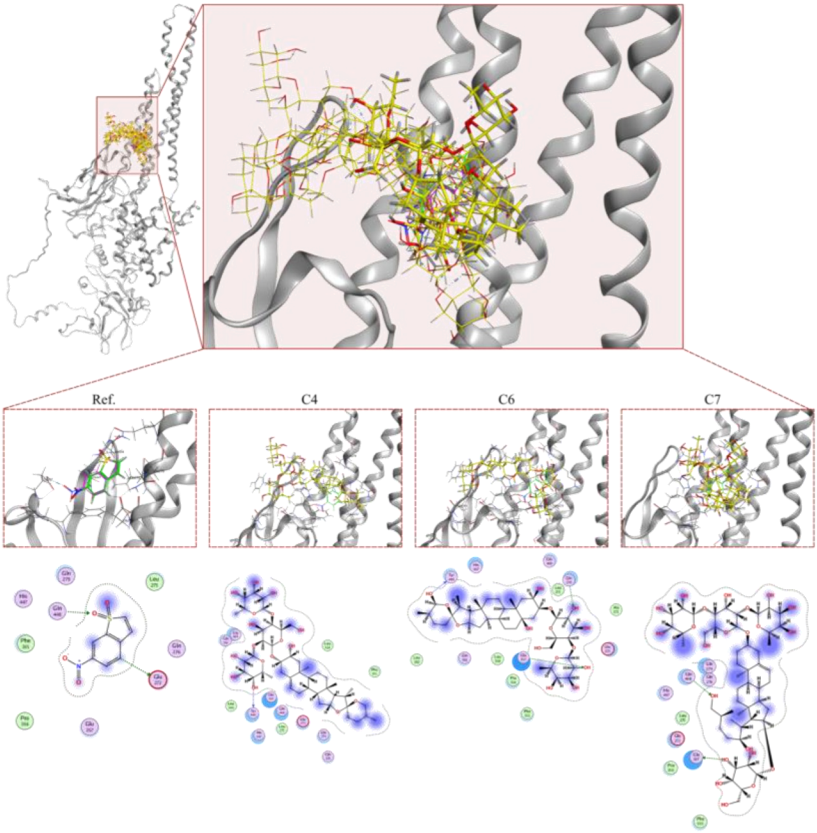


Fig. 4. Molecular docking visualization of several compound (C4, C6, and C7) and the reference ligand within the STAT3 binding pocket. The upper panel shows the overall binding region on the AlphaFold2-predicted STAT3 structure (gray ribbon), with the overlay of the DiffDock-predicted reference pose (magenta), the MOE-redocked reference pose (green), and the docked compounds (yellow). The lower panels present close-up binding orientations and corresponding two-dimensional interaction maps of the reference ligand and compounds C4, C6, and C7, demonstrating their localization within the same predicted binding region of STAT3.

This study has several limitations that should be acknowledged. As with any in silico-based study, the findings presented here require experimental confirmation. Target prediction and molecular docking results represent computational estimations rather than direct measurements of biological activity. Further in vitro antiplasmodial assays and in vivo validation are therefore needed to confirm the therapeutic potential of bioactive compounds identified in this study.

4 Conclusion

This study demonstrates that bioactive compounds from Allium tuberosum show potential as antimalarial agent candidates, based on their favorable ADMET screening profile, their broad overlap with malaria-associated targets through network pharmacology analysis, their convergence on STAT3 as a central hub gene linked to malaria-relevant inflammatory pathways, and their strong binding affinity toward STAT3 in molecular docking analysis. Among the tested compounds, C7 exhibited the most favorable binding profile, surpassing the reference compound. Nevertheless, further in vitro and in vivo validation is required to confirm the antimalarial efficacy of these compounds.

Acknowledgments. The authors gratefully acknowledge the Faculty of Medicine, State University of Malang, for providing financial support for the publication of this work.

Disclosure of Interests. The authors have no competing interests to declare that are relevant to the content of this article.

References

1. World Health Organization: World malaria report 2025: Addressing the threat of antimalarial drug resistance, https://www.who.int/teams/global-malaria-programme/reports/world-malaria-report-2025.
2. Kambuaya, N.N., Ramli, M.S.S., Candrawati, F., Kenangalem, E., Prayoga, P., Puspitasari, A.M., Noviyanti, R., Trianty, L., Indrawanti, R., Simatupang, M., Ubra, R.R., Hill, J., Hafidz, F., Poespoprodjo, J.R.: Treatment Efficacy of Dihydroartemisinin–Piperaquine for Uncomplicated Plasmodium falciparum and Plasmodium vivax Malaria in Timika, Papua, Indonesia. Am J Trop Med Hyg. 114, 115–122 (2026). https://doi.org/10.4269/ajtmh.25-0291.
3. Theodoridis, L., Carvalho, T.G.: Antimalarial drug resistance and drug discovery: learning from the past to innovate the future. International Journal for Parasitology: Drugs and Drug Resistance. 28, 100602 (2025). https://doi.org/10.1016/j.ijpddr.2025.100602.
4. Sanyaolu, A., Marinkovic, A., Prakash, S., Balendra, V., Shazley, O., Gardellini, T., Jan, A., Younis, K., Okorie, C., Izurieta, R.: Emerging Molecular Mechanisms in Malaria Pathogenesis and Novel Therapeutic Approaches: A Focus on P. falciparum Malaria. Biomolecules. 15, 1038 (2025). https://doi.org/10.3390/biom15071038.
5. Tobing, T.C.L., Wahrianto, Saputri, E., Wafa, N.I., Zulfianti, P.D., Sihaloho, L.I., Husna, A.R., Salsabila, D., Silalahi, F.H.H., Sitohang, A.I., Sabrina, A., Harianja, A.D.H., Barus, S.A., Sabina, S., Rahma, A.A., Velaro, A.J., Khairunnnisa, K., Salim, E., Nurkolis, F., Syahputra, R.A.: Malaria in Indonesia: current treatment approaches, future strategies, and potential herbal interventions. Pharmacia. 71, 1–14 (2024). https://doi.org/10.3897/pharmacia.71.e116095.
6. Nuryady, M.M., Juliana, L.I., Ariesaka, K.M.: In Silico Analysis of Active Compounds from Allium tuberosum as Drug Candidate for Inhibitor DENV-3 Envelope Protein. Jurnal ILMU DASAR. 25, 135 (2024). https://doi.org/10.19184/jid.v25i2.36400.

7. Petropoulos, S.A., Di Gioia, F., Polyzos, N., Tzortzakis, N.: Natural Antioxidants, Health Effects and Bioactive Properties of Wild Allium Species. Current Pharmaceutical Design. 26, 1816–1837 (2020). https://doi.org/10.2174/1381612826666200203145851.
8. Sutejo, I.R., Ariesaka, K.M., Prasetyo, F.A., Taufiqurrqhman, M., Insani, A.Y., Ariansari, B.G.: Immunostimulant Effect of Garlic Chives Leaf Ethanolic Extract (Allium tuberosum) by Increasing Level of Antioxidant at Rats Doxorubicin-Induced Rats. Indonesian Journal of Cancer Chemoprevention. 7, 93 (2017). https://doi.org/10.14499/indonesianjcanchemoprev7iss3pp93-98.
9. Nigussie, G., Wale, M.: Medicinal plants used in traditional treatment of malaria in Ethiopia: a review of ethnomedicine, anti-malarial and toxicity studies. Malar J. 21, 262 (2022). https://doi.org/10.1186/s12936-022-04264-w.
10. Merecz-Sadowska, A., Sadowski, A., Zielińska-Bliźniewska, H., Zajdel, K., Zajdel, R.: Network Pharmacology as a Tool to Investigate the Antioxidant and Anti-Inflammatory Potential of Plant Secondary Metabolites—A Review and Perspectives. International Journal of Molecular Sciences. 26, 6678 (2025). https://doi.org/10.3390/ijms26146678.
11. Corso, G., Stärk, H., Jing, B., Barzilay, R., Jaakkola, T.: DiffDock: Diffusion Steps, Twists, and Turns for Molecular Docking, http://arxiv.org/abs/2210.01776, (2023). https://doi.org/10.48550/arXiv.2210.01776.
12. Vasquez, M., Zuniga, M., Rodriguez, A.: Oxidative Stress and Pathogenesis in Malaria. Front Cell Infect Microbiol. 11, 768182 (2021). https://doi.org/10.3389/fcimb.2021.768182.
13. Colvin, H.N., Joice Cordy, R.: Insights into malaria pathogenesis gained from host metabolomics. PLoS Pathog. 16, e1008930 (2020). https://doi.org/10.1371/journal.ppat.1008930.
14. Dey, S., Mohapatra, S., Khokhar, M., Hassan, S., Pandey, R.K.: Extracellular Vesicles in Malaria: Shedding Light on Pathogenic Depths. ACS Infect Dis. 10, 827–844 (2024). https://doi.org/10.1021/acsinfecdis.3c00649.
15. Jin, P., Duan, X., Huang, Z., Dong, Y., Zhu, J., Guo, H., Tian, H., Zou, C.-G., Xie, K.: Nuclear receptors in health and disease: signaling pathways, biological functions and pharmaceutical interventions. Signal Transduct Target Ther. 10, 228 (2025). https://doi.org/10.1038/s41392-025-02270-3.
16. Chaudhary, A., Kataria, P., Surela, N., Das, J.: Pathophysiology of Cerebral Malaria: Implications of MSCs as A Regenerative Medicinal Tool. Bioengineering. 9, 263 (2022). https://doi.org/10.3390/bioengineering9060263.
17. Ndoricyimpaye, E.L., Van Snick, J., Niyoyita, J. de D., Kanimba, P., Mbonimpa, J.B., Rutayisire, R., Rutayisire, R., Ndahindwa, V., Cheou, P., Coutelier, J.P., Rujeni, N.: Integrated Analysis of Cytokine Profiles in Malaria Patients Discloses Selective Upregulation of TGF-β1, β3, and IL-9 in Mild Clinical Presentation. International Journal of Molecular Sciences. 23, 12665 (2022). https://doi.org/10.3390/ijms232012665.
18. Aggarwal, S., Karmakar, A., Krishnakumar, S., Paul, U., Singh, A., Banerjee, N., Laha, N., Ball, G.R., Srivastava, S.: Advances in Drug Discovery based on Genomics, Proteomics and Bioinformatics in Malaria. Current Topics in Medicinal Chemistry. 23, 551–578 (2023). https://doi.org/10.2174/1568026623666230418114455.
19. Mirdita, M., Schütze, K., Moriwaki, Y., Heo, L., Ovchinnikov, S., Steinegger, M.: ColabFold: making protein folding accessible to all. Nat Methods. 19, 679–682 (2022). https://doi.org/10.1038/s41592-022-01488-1.

Open Access This chapter is licensed under the terms of the Creative Commons Attribution-NonCommercial 4.0 International License (http://creativecommons.org/licenses/by-nc/4.0/), which permits any noncommercial use, sharing, adaptation, distribution and reproduction in any medium or format, as long as you give appropriate credit to the original author(s) and the source, provide a link to the Creative Commons license and indicate if changes were made.

The images or other third party material in this chapter are included in the chapter's Creative Commons license, unless indicated otherwise in a credit line to the material. If material is not included in the chapter's Creative Commons license and your intended use is not permitted by statutory regulation or exceeds the permitted use, you will need to obtain permission directly from the copyright holder.

